Effect of Array Geometry on the Capacity of the Turbo-Coded Beamforming Aided Uplink

S. Sugiura*, D. Yang†, S. Chen†, L.-L. Yang† and L. Hanzo†

*,†School of ECS, University of Southampton, SO17 1BJ, UK, Tel: +44-23-8059-3125, Fax: +44-23-8059-4508
Email: {ss07r,lh}@ecs.soton.ac.uk, http://www-mobile.ecs.soton.ac.uk
*TOYOTA Central R&D Labs., Inc., Aichi, 480-1192, Japan, Tel: +81-561-71-7163, Fax: +81-561-63-5258
Email: sugiura@mosk.tytlabs.co.jp, http://www.tytlabs.co.jp/eindex.html

Abstract—This paper investigates the effect of different array geometries on the performance of the turbo coding assisted beamforming uplink. More specifically, we focus on the maximum achievable rate as a measure of the system performance, which is calculated with the aid of EXIT chart analysis. Our performance results recorded for $K = 4$ uplink receiver antenna elements at the Base Station (BS) supporting $M = 4$ or $M = 7$ users demonstrated that the Hexagonal Array (HA) slightly outperforms the Uniform Linear Array (ULA) and Uniform Circular Array (UCA), when we have a low angular spread σ for the Direction-Of-Arrival (DOA) of each user. It is also demonstrated that the performance difference becomes smaller upon increasing the angular spread σ.

Index Terms—Array geometry, beamforming, capacity, turbo coding.

I. INTRODUCTION

The employment of multiple antenna elements at the transmitter and/or the receiver has the potential of substantially improving the achievable capacity and/or reliability of wireless links [1]. The most suitable Multiple-Input Multiple-Output (MIMO) configuration is typically dependent on the channel characteristics, the communication scenario and the system requirements.

Only limited attention has been paid to different array geometries, while considering their influence is important from the perspective of having a compact, light-weight ergonomic system design. In [2] the radiation patterns and the convergence characteristics of both a Uniform Circular Array (UCA) and of a Uniform Rectangular Array (URA) were investigated in the context of adaptive beamforming. Additionally, Tsai *et al.* [3] compared the Bit Error Ratio (BER) performance of UCA and ULA using Maximum Ratio Combining (MRC) under the time-varying Rayleigh fading environment for the simplified scenario, where only a single user is supported, i.e. without considering any interferences. Further studies have been conducted in [4], [5], focusing on the Continuous-input Continuous-output Memoryless Channel (CCMC) capacity of Spatial Division Multiplexing (SDM) for several array geometries, including the so-called star array and Hexagonal Array (HA).

However, the above-mentioned studies mainly focused on uncoded systems, although the practical communication sys-

tems typically employ a powerful channel coding scheme, such as turbo coding [6] or Low Density Parity Check (LDPC) coding [7], hence they tend to have quite different characteristics from those of the uncoded systems. *Against this background, the novel contribution of this paper is that we first characterize the performance of the different array geometries in the context of the turbo-coded beamforming aided UpLink (UL). More specifically, the maximum achievable rates of the coded system are investigated with the aid of EXtrinsic Information Transfer (EXIT) chart analysis* [8] *in several scenarios, including a rank-deficient one, where the number of UL receiver antenna elements is lower than the number of UL transmitters M.*

The remainder of this paper is organized as follows. Section II describes the array employed and the system model. In Section III, we provide our simulation results, while Section IV concludes the paper.

II. SYSTEM OVERVIEW

A. Array geometries

In this contribution we consider three different types of Base Station (BS) receiver array geometries, i.e. the ULA, the UCA and the HA. The K-element BS receiver array's steering vectors $\boldsymbol{a}(\phi,\theta) = [a_1(\phi,\theta),\cdots,a_K(\phi,\theta)]^T \in \mathcal{C}^{M\times 1}$ are expressed in Eq. (1)-(3) for the three arrays in the spherical polar coordinates (r, ϕ, θ), which are shown at the top of this page. Here, λ is the wavelength and D is the element-spacing for the ULA, while R is the radius of the UCA and the HA. For simplicity of notation we set $\theta = 90^o$ throughout this paper, since this choice was employed also in the previous studies of [2]-[5].

B. System description

Consider the turbo coding assisted beamforming uplink, where the BS is equipped with a K-element antenna array receiving from the M UL users, each having a single transmit antenna element, where the mth user is located in the direction of (ϕ_m, θ_m) from the BS. At each of the M users the source bits are first channel-encoded and then interleaved by the user-specific interleaver Π_m. The interleaved bits are mapped to the constellation symbols $s_m(t)$ $(m = 1,\cdots,M)$ depending on the modulation scheme employed. Finally, the M users simultaneously transmit their own symbols to the BS within the same time slot and frequency slot.

$$\boldsymbol{a}(\phi,\theta) = \left[1, \cdots, \exp\left\{j\frac{2\pi}{\lambda}D(K-1)\sin\phi\right\}\right]^T \quad (ULA) \tag{1}$$

$$\boldsymbol{a}(\phi,\theta) = \left[\exp\left\{j\frac{2\pi}{\lambda}R\sin\theta\cos\phi\right\}, \cdots, \exp\left\{j\frac{2\pi}{\lambda}R\sin\theta\cos\left(\phi - \frac{2\pi}{K}(k-1)\right)\right\},\right.$$
$$\left.\cdots, \exp\left\{j\frac{2\pi}{\lambda}R\sin\theta\cos\left(\phi - \frac{2\pi}{K}(K-1)\right)\right\}\right]^T \quad (UCA) \tag{2}$$

$$\boldsymbol{a}(\phi,\theta) = \left[1 \;\; \exp\left\{j\frac{2\pi}{\lambda}R\sin\theta\cos\phi\right\}, \cdots, \exp\left\{j\frac{2\pi}{\lambda}R\sin\theta\cos\left(\phi - \frac{2\pi}{K-1}(k-2)\right)\right\},\right.$$
$$\left.\cdots, \exp\left\{j\frac{2\pi}{\lambda}R\sin\theta\cos\left(\phi - \frac{2\pi}{K-1}(K-2)\right)\right\}\right]^T \quad (HA) \tag{3}$$

Furthermore, we assume that the channels between the mth user and the BS, which are expressed as $\boldsymbol{h}_m(t) = [h_{m1}(t), \cdots, h_{mK}(t)]^T \in \mathcal{C}^{K \times 1}$, are frequency-independent block Rayleigh fading channels, which are given by [3]

$$\boldsymbol{h}_m(t) = \frac{1}{\sqrt{L}}\sum_{l=1}^{L}\exp\left[j\left\{2\pi f_d\cos(\Psi_l)t + \Phi_l\right\}\right]\boldsymbol{a}(\phi_{ml}), \quad (4)$$

where L is the number of scatterers in the Jakes model, i.e. the number of paths arriving at each of the K UL antenna elements at the same instance. Moreover, Φ_l is the random phase and Ψ_l is the random Direction-Of-Departure (DOD), both of which are uniformly distributed between 0° to 360°, while f_d is the maximum Doppler frequency. Each Direction-Of-Arrival (DOA) of the L paths ϕ_{ml} $(l = 1, \cdots, L)$ between the mth user and the BS is generated based on the Gaussian distribution having the mean of ϕ_m and the standard derivation σ, which is also referred to as the angular spread in this contribution.

At the BS the received signals $\boldsymbol{y}(t) \in \mathcal{C}^{K \times 1}$ are given by

$$\begin{aligned}\boldsymbol{y}(t) &= [y_1(t), \cdots, y_K(t)]^T \\ &= \sum_{m=1}^{M}\boldsymbol{h}_m(t)s_m(t) + \boldsymbol{n}(t),\end{aligned} \tag{5}$$

where $\boldsymbol{n}(t) = [n_1(t), \cdots, n_K(t)]^T \in \mathcal{C}^{K \times 1}$ is the noise vector, whose components have zero mean and a variance of $2\sigma_n^2$. The receiver employs iterative detection based on the turbo principle, where the mutual information is iteratively exchanged between two Soft-Input Soft-Output (SISO) decoders, namely the SISO Interference Cancellation (IC) aided Multi-User Detection (MUD) and the M number of parallel single-user SISO channel decoders. After a certain number of extrinsic information exchanges via user-specific interleavers/deinterleavers, the estimated bits are output by the channel decoders. More specifically, at the SISO-IC aided MUD the symbols received from each user are classified on the basis of the beamforming concept, where the undesired symbols are ...ly filtered out by the antenna radiation pattern, depending on the user-specific DOAs. For example, the MUD can utilize the Zero Forcing (ZF) scheme, the Minimum Mean Square Error (MMSE) scheme [9], the Minimum Bit Error Rate (MBER) scheme [10] and so on.

TABLE I
BASIC SYSTEM PARAMETERS

Number of UL users M	4. 7
Number of Rx antenna elements K	4
Rx antenna array type	ULA, UCA, HA
Modulation Scheme	QPSK, 16-QAM
Channel	Frequency flat Rayleigh fading channel
Number of scatterers L	50
Angular spread σ	1°–50°
DOAs $(\phi_1, \cdots, \phi_K)$	Fixed $(30^o,\ 0^o,\ 280^o, 335^o)$ or Uniformly random
Outer channel code	1/2-rate convolutional code
Interleaver block length	10 000 bits
SISO-IC aided MUD	MMSE

III. SYSTEM PERFORMANCE

In this section we discuss our performance results recorded for the three different types of array geometries, i.e. for the ULA, the UCA and the HA. The basic system parameters employed in the simulations are listed in Table I. It is assumed that each array is equipped with K = 4 antenna elements and that the popular SISO-IC aided MMSE MUD [9] is employed for the inner decoder of the receiver. For simplicity, we also assumed vehicular speed of zero, which eliminates the Doppler effect, yielding f_d = 0. The number of scatterers was L = 50. Furthermore, the interleaver length of each user was set to 10 000 bits and the channel components of $\boldsymbol{h}_m(t)$ ($m = 1, \cdots, M$) were assumed to be perfectly estimated at the BS.

Fig. 1 shows the EXIT curves of the three different arrays supporting M = 4 users having the DOAs of $(\phi_1, \cdots, \phi_4) = (30^o,\ 0^o,\ 280^o, 335^o)$ at the Eb/N0 = 0, 10 and 20 dB, where 16QAM was employed as our modulation scheme. Note that the EXIT curves corresponding to all the users were averaged here, assuming the same power for the M = 4 UL transmitters, because we are unable to visualize a five-dimensional EXIT chart, which would be required for four users. Observe in Fig. 1 that while all the three EXIT curves are similar at the Eb/N0 = 0 dB, the performance advantage of the HA increases upon
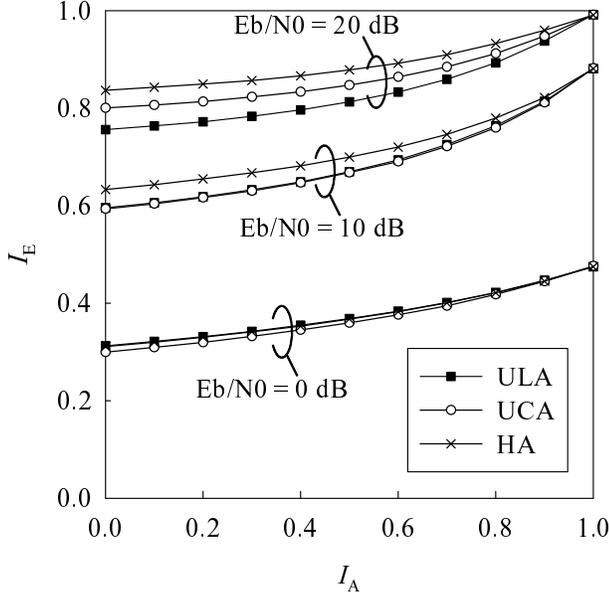
Fig. 1. EXIT curves of the three different array geometries, i.e. the ULA, the UCA and the HA, having $K = 4$ antenna elements at the Eb/N0 = 0, 10 and 20 dB, where the $M = 4$ users with the DOAs $(\phi_1, \cdots, \phi_4) = (30^o, 0^o, 280^o, 335^o)$ are supported.
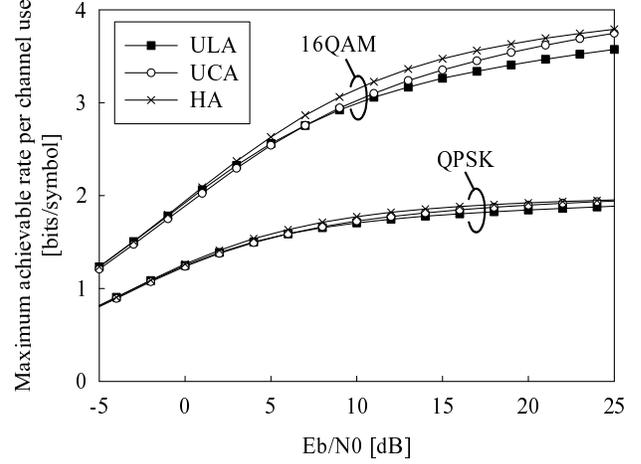

Fig. 2. Maximum achievable rates of the three different arrays having $K = 4$ antenna elements and supporting $M = 4$ QPSK- or 16QAM-modulated users.
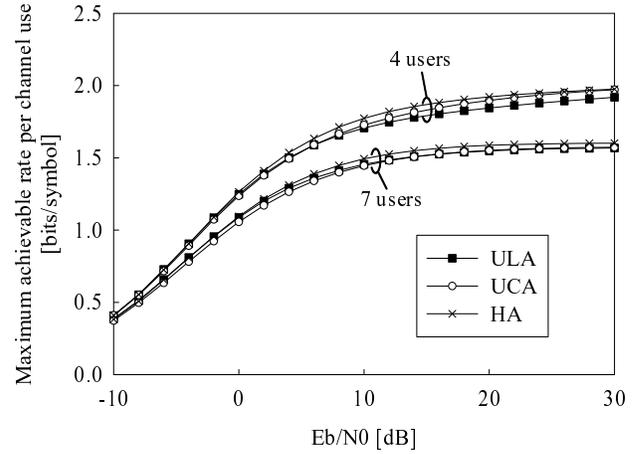

Fig. 3. Maximum achievable rates in full-rank and rank-deficient beamforming uplink having $K = 4$ antenna elements, where $M = 4$ and $M = 7$ QPSK-modulated users are supported, respectively.

increasing the Eb/N0 value. This indicates that the HA reaches the turbo cliff at a slightly lower Eb/N0 or with a potentially lower number of iterations than the other two arrays due to its wider open area between the inner and outer codes' EXIT curves.

Next, we investigated the maximum achievable rates of the beamforming uplink, which are calculated based on our results of the EXIT chart analysis. It was shown in [11] that the approximate maximum achievable rate R can be expressed as

$$R(\rho) = \log_2(\mathcal{M})A(\rho), \qquad (6)$$

where $A(\rho)$ corresponds to the area under the EXIT curve at a certain value of Eb/N0 = ρ and $\mathcal{M}$ is the constellation size employed. It should be noted that the maximum achievable rate of coded systems may be determined by EXIT chart analysis for comparison to the unrestricted CCMC capacity, which was used as a performance measure in the previously-studied uncoded systems [4], [5]. This is because the maximum achievable rate takes into account the effect of the specific modulation scheme employed.

Fig. 2 shows the maximum achievable rates of the three different arrays, where $M = 4$ QPSK- or 16QAM-modulated users are supported. In the rest of this paper 100 random DOA cases $(\phi_1, \cdots, \phi_4)$ are generated to calculate the maximum achievable rates, while the angular spread σ is set to $\sigma = 1^o$. It is shown in Fig. 2 that for 16QAM the HA exhibited a marginally better maximum achievable rate than the UCA followed by the ULA. It can be also said that for QPSK the HA slightly outperformed the other two arrays, but its performance advantage became smaller compared to the 16QAM case.

Additionally, Fig. 3 investigated the maximum achievable

rates of both the full-rank scenario and of a rank-deficient scenario, where $M = 4$ and $M = 7$ QPSK-modulated users were supported, while the other parameters remained the same as those used in Fig. 2. As expected, the maximum achievable per-channel-use rate of the $M = 7$-user scenario was degraded in comparison to that of $M = 4$ users, but nevertheless we may conclude that the turbo-coded systems have the capability of operating in a rank-deficient scenario. In fact, it may be argued that the 4-user system had a total throughput of $4 \times 2 = 8$ bits/symbol, while the 7-user system had $7 \times 1.6 = 11.2$ bits/symbol, or half of these values, when considering the half-rate Forward Error Correction (FEC) code. In both cases the HA exhibits a slightly better performance than the other two arrays.

Finally, we investigated the effect of the angular spread σ on the achievable system performance of each array. Fig. 4 plots the Eb/N0, at which 90% of the throughput upper
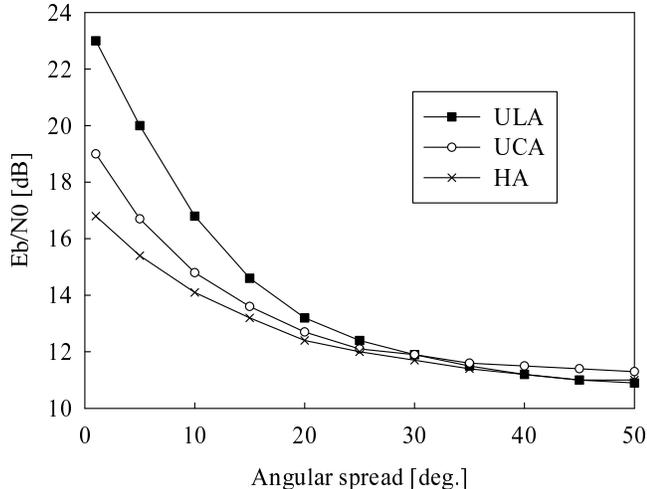
Fig. 4. Effect of angular spread σ on the Eb/N0, at which the system maximum achievable rate achieves 90% of the upper bound.

bound is achieved, versus the angular spread σ, where $M = 4$ 16QAM-modulated users are supported. Note that in this 16QAM case the 90% throughput upper bound corresponds to 3.6 bits/symbol. Observe in Fig. 4 that for $\sigma = 1^o$ the HA achieved a 2 dB better performance than the UCA and 6 dB better than the ULA. However, upon increasing the angular spread σ, this advantage of the HA becomes negligible. This is because for the small angular spreads σ each user is uniquely identified with the aid of the beamforming concept, the success of which is based on the user-specific DOAs, where the K channel components $\boldsymbol{h}_m(t)$ for each user are mutually correlated to a different extent depending on the array geometry and on the DOAs. On the other hand, for large angular spreads σ each user is essentially separated based on the user-specific Channel Impulse Responses (CIRs), where the concept becomes Space Division Multiple Access (SDMA) rather than beamforming [1]. This results in a reduced performance difference for the arrays due to the fact that the CIRs $\boldsymbol{h}_m(t)$ of the users exhibit a low correlation and hence the channel matrix $\boldsymbol{H} = [\boldsymbol{h}_1(t), \cdots, \boldsymbol{h}_M(t)]$ approaches the condition of having a full-rank.

IV. CONCLUSION

In this paper we presented the impact of three different array geometries, i.e. that of the ULA, the UCA and the HA, on the maximum achievable rate in the context of the turbo-coded beamforming uplink. Our performance results for $K = 4$ antenna elements demonstrated that the HA outperformed the other two arrays in case of small angular spread σ both for the $M = 4$-user full-rank scenario and for the $M = 7$-user rank-deficient scenario. It was also demonstrated that the performance difference became marginal upon increasing the angular spread σ.

REFERENCES

[1] L. Hanzo, O. Alamri, M. El-Hajjar, and N. Wu, *Near-Capacity Multi Functional MIMO Systems*. John Wiley and IEEE Press, 2009.
[2] P. Ioannides and C. Balanis, "Uniform circular and rectangular arrays for adaptive beamforming applications," *IEEE Antennas and Wireless Propagation Letters*, vol. 4, pp. 351–354, 2005.
[3] J. Tsai, R. Buehrer, and B. Woerner, "BER performance of a uniform circular array versus a uniform linear array in a mobile radio environment," *IEEE Transactions on Wireless Communications*, vol. 3, no. 3, pp. 695–700, 2004.
[4] A. Forenza and R. Heath Jr, "Impact of antenna geometry on MIMO communication in indoor clustered channels," in *IEEE Antennas and Propagation Society International Symposium*, vol. 2, Monterey, CA, USA, 20–25 June 2004, pp. 1700–1703.
[5] R. Bhagavatula, R. Heath, S. Vishwanath, and A. Forenza, "Sizing up MIMO arrays," *IEEE Vehicular Technology Magazine*, vol. 3, no. 4, pp. 31–38, 2008.
[6] L. Hanzo, T. Liew, and B. Yeap, *Turbo coding, turbo equalisation and space-time coding for transmission over fading channels*. John Wiley and IEEE Press, 2002.
[7] T. Richardson and R. Urbanke, "The capacity of low-density parity-check codes under message-passing decoding," *IEEE Transactions on Information Theory*, vol. 47, no. 2, pp. 599–618, 2001.
[8] S. ten Brink, "Convergence behavior of iteratively decoded parallel concatenated codes," *IEEE Transactions on Communications*, vol. 49, no. 10, pp. 1727–1737, 2001.
[9] X. Wang and H. Poor, "Iterative (turbo) soft interference cancellation and decoding for coded CDMA," *IEEE Transactions on Communications*, vol. 47, no. 7, pp. 1046–1061, 1999.
[10] S. Sugiura, S. Chen, and L. Hanzo, "Reduced-complexity iterative Markov chain MBER detection for MIMO systems," *IEEE Signal Processing Letters*, vol. 16, no. 3, pp. 160–163, 2009.
[11] M. Tüchler, "Design of serially concatenated systems depending on the block length," *IEEE Transactions on Communications*, vol. 52, no. 2, pp. 209–218, 2004.